The pivot algorithm and polygons: results on the FCC lattice

1990 J. Phys. A: Math. Gen. 23 1589

(http://iopscience.iop.org/0305-4470/23/9/021)

J. Phys. A: Math. Gen. 23 (1990) 1589-1612. Printed in the UK

The pivot algorithm and polygons: results on the FCC lattice

E J Janse van Rensburg†, S G Whittington† and N Madras‡

† Department of Chemistry, University of Toronto, Toronto, Ontario, M5S 1A1, Canada
‡ Department of Mathematics, York University, 4700 Keele Street, North York, Ontario, M3J 1P3, Canada

Received 14 September 1989, in final form 9 November 1989

Abstract. We consider the pivot algorithm for polygons on the face-centred cubic lattice and prove ergodicity. A numerical study of the algorithm is carried out; in particular, we look at the acceptance fraction of the elementary moves and find that it goes only slowly to zero as the length of the polygons is increased. The numerical properties of polygons on the FCC lattice are also considered. We calculate the exponent ν (by considering the mean square radius of gyration of the polygons) and compare the result to the expected value (from field theory). We also consider the mean span of the polygons and discuss corrections to scaling and their influence on the numerical calculation of critical exponents.

1. Introduction

The numerical simulation of the self-avoiding walk has received much attention in recent years. The reasons for the popularity of this model are its simplicity, and its close relation to complex problems in chemistry (as a model for polymers), physics (due to its relation to the $(n=0)$ n-vector model) and mathematics (as an example of a non-Markov probability model).

Over the last thirty years, progress in the simulation of self-avoiding walks has been steady, due to the improvement in computer technology, and also due to the invention of more effective algorithms. Lal (1969) invented an interesting algorithm for the simulation of self-avoiding walks in the canonical ensemble which was used by Olaj and Pelinka (1976) and rediscovered by MacDonald *et al* (1985). Apart from these studies, the algorithm received little attention until it was studied in detail by Madras and Sokal (1988), who called it the pivot algorithm and showed that it is extraordinarily efficient in the simulation of self-avoiding walks. Continuum versions of the pivot algorithm can be found in the work of Stellman and Gans (1972a, b) and of Freire and Horta (1976).

While there has been significant development in the simulation of self-avoiding walks in the canonical ensemble since the early 1960s, it is only recently that significant progress has been made in the simulation of polygons (we define a polygon to be a walk which starts and ends at the origin, and is otherwise self-avoiding). The interest in polygons goes back to about 1960 (Hammersley 1961, Kesten 1963). The numerical simulation of polygons proved more difficult than that of walks, mainly due to the absence of effective algorithms. This state of affairs frustrated the numerical studies of closed polymer chains on the lattice with specific application in, for example, biology (Frank-Kamenetskii *et al* 1975, Michels and Wiegel 1986 and Sumners 1987). Most results on polygons come from exact enumeration studies. Here, the effort was concentrated on the square and cubic lattice (Martin *et al* 1967, Privman and Rudnick 1985,

0305-4470/90/091589+24$03.50

Guttmann and Enting 1988) although the honeycomb lattice (Enting and Guttmann 1989) and the face-centred cubic (FCC) lattice (Rapaport 1975) also received attention.

Madras *et al* (1989) proved that a 'pivot algorithm' can be applied to polygons on the cubic lattice, extending the two-dimensional result of Dubins *et al* (1988). In this paper we set out to study the properties of the pivot algorithm for polygons on the FCC lattice. To prove that the algorithm is ergodic on the FCC lattice is an interesting problem which we address in this paper. We are also interested in the numerical properties of the algorithm. In particular, we look at the acceptance fraction (f) of the proposed elementary moves and the autocorrelations of several observables.

We also study the properties of polygons on the FCC lattice. Of particular interest are scaling exponents, and corrections to scaling. The numerical values of the scaling exponents were calculated using field theory methods (Le Guillou and Zinn-Justin 1980, 1989), and we can compare our results to those predictions. We consider polygons of length almost 3000 edges, enabling us to expose the scaling behaviour of the quantities that we calculate.

This paper is organised as follows. In section 2 we describe the algorithm. In particular, we define the elementary pivot transformations of the algorithm and discuss their reversibility. In section 3 we prove that the algorithm is ergodic on the FCC lattice provided that a certain set of elementary transformations have non-zero probability of occurring. The initialisation of the algorithm is discussed in section 4. Furthermore, we look at the relative frequencies of successful elementary transformations as we increase the number of vertices in the polygon (n). The acceptance fraction (f) of the algorithm is known to go to zero as n goes to infinity, but our numerical data imply that this happens only slowly. In fact we expect that $f \sim n^{-p}$ where p is a small number, and we find $p = 0.247 \pm 0.004 \pm 0.001$ (where the format is $p \pm$ systematic error $\pm$ statistical error, the statistical error is the 95% confidence limits). The computational efficiency of the algorithm is also considered. We define the mean amount of work per attempted transformation and find that it increases as n^w, where the numerical data indicate that $w = 0.858 \pm 0.001 \pm 0.002$.

In section 5 we consider the properties of polygons on the FCC lattice. We calculate four global quantities and their autocorrelations: the mean square radius of gyration, the mean span, the mean fourth moment of the radius of gyration and the mean of the square span divided by the square radius of gyration. A least-squares analysis of the radius of gyration data gives $\nu = 0.593 \pm 0.003 \pm 0.002$, close to the value found by Madras and Sokal (1988) for the self-avoiding walk. We show that the MC data are consistent with the field theory value $\nu = 0.588 \pm 0.002$ if there is a correction-to-scaling exponent $\Delta = 0.470 \pm 0.025$. We also consider the span of the polygons; we find large corrections to scaling, so that it is impossible to find a good estimate for ν from these data.

Assuming the field theory values of the critical exponents, it is possible to calculate the amplitudes of the mean square radius of gyration and the mean span. The belief that there is only one length scale in this problem can be tested by considering a ratio of the span and the radius of gyration of the polygons. We consider the mean of the square span divided by the square radius of gyration, which we believe will depend on n as

$$\left\langle \frac{s^2}{r^2} \right\rangle_n = \alpha + \beta n^{-\Delta} + \gamma n^{-1} + \ldots \tag{1.1}$$

where s is the span and r^2 is the square radius of gyration of the polygon. α is believed

to be lattice independent. If we assume that $\Delta = 0.47$, then a least-squares analysis gives $\alpha = 5.69 \pm 0.02$ (95% confidence limits). We also consider the mean fourth moment of the radius of gyration, $\langle r^4 \rangle$. If we assume that for large n it scales as n^{γ_4}, then our best estimate for this critical exponent is $2.375 \pm 0.004 \pm 0.004$. This number is, to a good approximation, equal to 4ν (see also Rapaport 1975). We end the paper with a few conclusions in section 6.

2. The pivot algorithm for polygons on the FCC lattice

A *polygon*, or *self-avoiding polygon*, is defined to be a sequence of lattice sites ω_0, $\omega_1, \ldots, \omega_n$, and associated edges, such that: $\omega_0 = \omega_n$, ω_i and ω_{i+1} are neighbours in the lattice, and $\omega_1, \omega_2, \ldots, \omega_n$ are all distinct. In two dimensions, a *convex polygon* refers to the following classical geometrical object: a finite union of straight line segments which forms the boundary of a convex subset of the plane.

The basic elementary move of the algorithm is as follows. Choose two different pivots (vertices of the current polygon) at random with (for example) a uniform distribution (this is a sufficient condition, but not necessary), say r_1 and r_2. This can be done in $\frac{1}{2}n(n-1)$ ways. With these pivots, apply an elementary transformation from a list of possible transformations to the shorter piece of the polygon (or alternatively, to the piece not containing the origin). If the result is a self-avoiding polygon then it is accepted, becoming the current polygon. Otherwise it is rejected, and the current polygon does not change.

2.1. Elementary transformations

Let $\{\boldsymbol{e}_i\}$ be the three orthogonal unit vectors in $\mathbb{Z}^3$ ($\boldsymbol{e}_1 = (1, 0, 0)$, $\boldsymbol{e}_2 = (0, 1, 0)$ and $\boldsymbol{e}_3 = (0, 0, 1)$). In this paper, we view the FCC as a sublattice of $\mathbb{Z}^3$ generated by the three primitive vectors $(\boldsymbol{e}_1 + \boldsymbol{e}_2)$, $(\boldsymbol{e}_1 + \boldsymbol{e}_3)$ and $(\boldsymbol{e}_2 + \boldsymbol{e}_3)$. In this description, the FCC has coordination number 12 and edges of length $\sqrt{2}$. We define the principal axes of the FCC as those of $\mathbb{Z}^3$, generated by the vectors $\boldsymbol{e}_i$, and the lattice planes as those planes generated by pairs of vectors $(\boldsymbol{e}_i, \boldsymbol{e}_j)$. We can also define planes inclined at 45° to two of the three lattice planes; these are generated by the vectors $(\boldsymbol{e}_i \pm \boldsymbol{e}_j, \boldsymbol{e}_k)$ with i, j, k all unequal, and are called 45° planes.

The possible elementary transformations are given by the octahedral group, which is the symmetry group of the cubic lattices. For ergodicity we do not need all the possible transformations, but only a few, as we shall show in section 3. In our numerical simulation we considered only the following transformations: point reflections (inversion), reflections through lattice planes, reflections through 45° planes and 90° rotations about lattice axes. In each case the 'origin' of the transformation is taken to be the midpoint of the line segment joining the two pivots. With each possible pair of pivots it may not be possible to perform all the transformations. For example, if the two pivots are on the same principal axis, then we can perform an inversion, or one of three possible lattice plane reflections, or one of two possible 45°-plane reflections or one of two possible 90° rotations; if the two pivots are on the same lattice plane, then we can perform either an inversion or a lattice plane reflection; and so on.

Let the coordinates of the vertex ω_m (in $\mathbb{Z}^3$) be $\omega_m = (x(\omega_m), y(\omega_m), z(\omega_m))$. Suppose that $r_1 < r_2$ are the chosen pivots on a polygon ω. Firstly, an inversion of the segment

of the polygon between the two pivots defines a new configuration

$$\omega'_m = \begin{cases} \omega_m & \text{if } m \leqslant r_1 \text{ or } m \geqslant r_2 \\ \omega_{r_1} + \omega_{r_2} - \omega_{r_1+r_2-m} & \text{if } r_1 < m < r_2. \end{cases} \tag{2.1}$$

Since the pivots are left unchanged, it is always possible to attempt an inversion. Secondly, a 90° rotation about the e_k axis is possible if the two pivots are both on this axis. The rotation may be either clockwise or anti-clockwise; we refer to a 90° rotation or a −90° rotation. The third and fourth possibilities are 45°-plane reflections and lattice plane reflections. For these to be possible, either ω_{r_1} and ω_{r_2} must both be in the plane of reflection, or else ω_{r_1} must be the image of ω_{r_2} under the reflection.

We shall now discuss detailed balance for the algorithm. For any given polygon ω and any two given pivots r_1 and r_2, we have in general several possible elementary moves that we may attempt. Let $\rho(t; x, y)$ be the probability of attempting the elementary transition t given that the pivots are at sites x and y. Observe that for each t, ρ depends only on the relative locations of x and y (i.e., whether they lie on the same principal axis, or on the same 45° plane, etc). Suppose that ω and ω' are n-step polygons such that ω' can be obtained from ω by the transformation t with pivots r_1 and r_2. Then the probability of going from ω to ω' via transformation t is equal to $p(r_1, r_2)\rho(t; \omega_{r_1}, \omega_{r_2})$, where $p(r_1, r_2)$ is the probability of choosing r_1 and r_2 as pivots (e.g., in the uniform case, $p(r_1, r_2) = 2/n(n-1)$). Since ω'_{r_1}, ω'_{r_2} is the same pair of points as ω_{r_1}, ω_{r_2} (possibly interchanged), it follows that $\rho(t; \omega_{r_1}, \omega_{r_2}) = \rho(t; \omega'_{r_1}, \omega'_{r_2})$. Note that every elementary transformation, except for 90° rotations, is its own inverse. The inverse of a 90° rotation is a −90° rotation. To have detailed balance, we have to put the probability of a 90° rotation equal to that of a −90° rotation. This means that $\rho(t, x, y) = \rho(t^{-1}, x, y)$, and so $p(r_1, r_2)\rho(t; \omega_{r_1}, \omega_{r_2}) = p(r_1, r_2)\rho(t^{-1}; \omega'_{r_1}, \omega'_{r_2})$. Therefore, summing over all r_1 and r_2, and t that transform ω into ω', we conclude that $p(\omega \to \omega') = p(\omega' \to \omega)$.

In simulations in this paper, $p(r_1, r_2)$ is uniform, and $\rho(t; x, y)$ is the reciprocal of the possible number of elementary moves for the pivots at x and y. (Another easily implemented scheme, though less efficient, would be to take ρ independent of x and y.)

Once a new configuration is proposed by the elementary moves it is accepted into the ensemble if it is self-avoiding. The most efficient way of checking the self-avoiding condition is through the use of a data structure known as a 'hash table' (Knuth 1973, Horowitz and Sahni 1976), as set out in Madras and Sokal (1988).

2.2. Description of the algorithm

The pivot algorithm for polygons is a MC algorithm (Metropolis *et al* 1953) simulating polygons in the canonical ensemble (with a fixed number, n, of vertices). Let R_n be the set of all polygons with n vertices, one vertex fixed at the origin. Let the cardinality of R_n be p_n. Then it is believed that

$$p_n \sim n^{\alpha_{\text{sing}}-2}\mu^n \tag{2.2}$$

where μ is the effective coordination number of the lattice, and α_{sing} is the specific heat critical exponent. An equal weight is assigned to each polygon in R_n. The algorithm has a finite state space R_n and an invariant probability measure

$$\pi_\omega = p_n^{-1} \qquad \forall \omega \in R_n. \tag{2.3}$$

The basic elementary transition is described by a transition probability matrix $\mathbf{P} = \{p(\omega \to \nu)\} = \{p_{\omega\nu}\}$ which has the following properties. (i) For each ω, $\nu \in R_n$ there exists an $m \geq 0$ such that the m-step transition probability from ω to ν, $p_{\omega\nu}(m)$, is positive. This is called ergodicity; we prove it in section 3. (ii) For each polygon $\omega \in R_n$, $\Sigma_{\omega \in R_n} \pi_\omega p_{\omega\nu} = \pi_\nu$. This is true for the pivot algorithm where π_ω is defined by equation (2.3).

Should these conditions be true, then it can be shown that π_ω is the unique limit distribution of the Markov chain with state space R_n and transition probability matrix $\mathbf{P}$ (Kemeny and Snell 1976). Let the observed states of the Markov chain be represented by X_i. The states X_i and X_j are in general correlated, so that the calculation of error bars of a real-valued function $A(\omega)$, $\omega \in R_n$, is a complicated procedure. If we start the Markov chain in equilibrium then $\{A_t\} = \{A(X_t)\}$ is a stationary stochastic process with mean

$$\langle A_t \rangle = \sum_{\omega \in R_n} \pi_\omega A(\omega) \tag{2.4}$$

and unnormalised autocorrelation function

$$C_{AA}(s) = \langle A_t A_{t+s} \rangle - \langle A_t \rangle^2. \tag{2.5}$$

We define the normalised autocorrelation

$$\rho_{AA}(t) = \frac{C_{AA}(t)}{C_{AA}(0)}. \tag{2.6}$$

Once the distribution is in equilibrium, we define the *integrated autocorrelation time* τ_{int}. This autocorrelation time controls the statistical error in MC measurements of $\langle A_t \rangle$. It is defined by

$$\tau_{\text{int}}(A) = \frac{1}{2} \sum_{t=-\infty}^{\infty} \rho_{AA}(t) \tag{2.7}$$

and the variance in the sample mean, A, over N observations, is asymptotically

$$\sigma^2(A) \sim \frac{1}{N} (2\tau_{\text{int}}(A)) C_{AA}(0). \tag{2.8}$$

In other words, the effective number of independent observations is $N/2\tau_{\text{int}}(A)$.

3. Ergodicity

We split the proof of ergodicity into two parts. First we prove that the algorithm is ergodic in a two-dimensional sublattice of the FCC, then we prove ergodicity in three dimensions. We begin with a few definitions and by defining some notation.

Let Π_0 be the plane in $\mathbb{R}^3$ generated by the unit vectors $\boldsymbol{e}_1$ and $\boldsymbol{e}_2$. Then $\Pi_0 \cap \text{FCC} = 2\mathbb{Z}^2$ (where the vertex set of $2\mathbb{Z}^2$ is $\{(x, y) \in \mathbb{Z}^2 | x + y \text{ is even}\}$) is a sublattice of the FCC which is the square lattice with edge length $\sqrt{2}$. We shall also consider projections of the FCC onto Π_0. If we define the dual of $2\mathbb{Z}^2$ to be $(2\mathbb{Z}^2)^*$, then all the vertices of the FCC are projected onto the vertices of the lattice $2\mathbb{Z}^2 \cup (2\mathbb{Z}^2)^*$, while the edges are projected onto edges of length $\sqrt{2}$ if they connect vertices in either $2\mathbb{Z}^2$ or in its dual, or onto edges of length 1 if they connect a vertex in $2\mathbb{Z}^2$ to a vertex in the dual lattice. This situation is illustrated in figure 1.

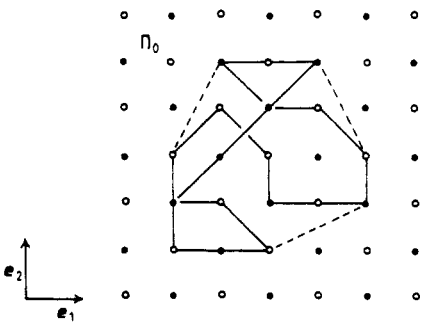

Figure 1. The projection of a polygon on the plane Π_0. The full circles are elements of the lattice $2\mathbb{Z}^2$ while the open circles represent the dual of $2\mathbb{Z}^2$. The convex hull of the projection is also indicated.

3.1. Ergodicity in the lattice $2\mathbb{Z}^2$

Only a polygon with an even number of vertices can be embedded in $2\mathbb{Z}^2$. If a polygon has an odd number of vertices, then we can put each vertex of the polygon, except for one, in this lattice; the last vertex can be left in the plane with third component just above or below a dual vertex in Π_0. It is easy to see that this odd vertex can be moved around at will by applying inversions and lattice-plane reflections. We say that a polygon with n vertices is *flat* if all its vertices are in Π_0 if n is even, or if at most one of its vertices is not in Π_0 if n is odd.

It is enough to consider only polygons with an even number of vertices confined to the sublattice $2\mathbb{Z}^2$. Dubins *et al* (1988) proved ergodicity of the pivot algorithm in two dimensions on the square lattice. We note that all we have to do is to interchange our definitions of lattice plane and 45° plane to get to their definitions, since our axes are at a 45° angle relative to theirs. So we immediately have the following lemma.

Lemma 3.1 (Dubins et al 1988). If inversion and reflections through lattice planes are given non-zero probability on the sublattice $2\mathbb{Z}^2$ (with axes defined as above) of the FCC, then the pivot algorithm is ergodic for all polygons confined to this sublattice. Furthermore, at most n transitions are needed to connect any two such polygons.

Combining this result with the arguments on polygons with odd numbers of vertices provides us with a proof of ergodicity for flat polygons. (However, when n is odd, we need $2n$ transitions to connect any two polygons.)

3.2. Ergodicity on the FCC

So far we have viewed the projection of the FCC on the plane Π_0 as the union of the lattice $2\mathbb{Z}^2$ and its dual. It is convenient to consider the FCC as the lattice generated by alternatively stacking copies of $2\mathbb{Z}^2$ and $(2\mathbb{Z}^2)^*$ on each other, each copy with the third component an integer. Each vertex in the FCC has twelve nearest neighbours, four in the copy of $2\mathbb{Z}^2$ to which it belongs, and four each in the dual lattices $(2\mathbb{Z}^2)^*$ in the planes above and below it.

Suppose that ω is a polygon in the FCC. The first, second and third coordinates of a vertex ω_i on ω will be denoted by $x(\omega_i)$, $y(\omega_i)$ and $z(\omega_i)$. Let $P\omega$ be the projection on the plane Π_0. In general, $P\omega$ is a loop on the lattice $2\mathbb{Z}^2 \cup (2\mathbb{Z}^2)^*$ $(=\Lambda)$, which may intersect itself, as illustrated in figure 1. We now need the following definition.

Definition 3.2. If the projection $P\omega$ of a polygon ω is a convex polygon on Λ, and if every $x \in P\omega$ is the image of a unique $x' \in \omega$ under the projection, then we say that ω is in *standard form.* We illustrate a polygon in standard form in figure 2. A little reflection indicates that a convex polygon on the lattice Λ has at least three and at most eight sides.

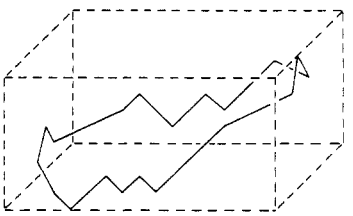

Figure 2. A polygon in standard form.

Notation. If $i<j$, then $[\omega_i : \omega_j]$ denotes the segment of the polygon containing $\omega_i, \omega_{i+1}, \ldots, \omega_j$, if $i>j$, then $[\omega_i : \omega_j]$ denotes the piece of ω which is the union of $[\omega_i : \omega_n]$ and $[\omega_0 : \omega_j]$.

Note that if $[\omega_i : \omega_j]$ is not a straight line segment, then its projection $P[\omega_i : \omega_j]$ can only be straight if $[\omega_i : \omega_j]$ is confined to a plane perpendicular to Π_0 and normal to either the axis $\boldsymbol{e}_1$ or the axis $\boldsymbol{e}_2$. If the projection of a segment is straight and inclined at 45° to a lattice axis, then the segment itself has to be straight by the geometry of the FCC.

Suppose that ω is a polygon that is not in standard form. (We shall deal later with standard polygons.) Consider $P\omega$, the projection of ω on the plane Π_0 (figure 1). Let $\mathscr{H}(\omega)$ be the boundary of the convex hull of $P\omega$ in the plane Π_0. Observe that if $\mathscr{H}(\omega)$ is a line segment, then a 45°-plane reflection, or a 90° rotation, of the entire polygon reduces the problem to lemma 3.1; thus henceforth we will assume that $\mathscr{H}(\omega)$ is a non-trivial convex polygon. We define the interior of $P\omega$, $\mathrm{Int}(\omega)$, to be all those points in Π_0 which cannot be connected to infinity by a curve in Π_0 that never intersects $P\omega$. Let

$$\alpha(\omega) = \mathrm{Area}\{\mathrm{Int}(\omega)\} \tag{3.1}$$

be the area of $\mathrm{Int}(\omega)$. We define the exterior of $P\omega$, $\mathrm{Ext}(\omega)$, to be the set $\Pi_0 - (\mathrm{Int}(\omega) \cup P\omega)$. The 'height' of ω, perpendicular to Π_0, will also play a useful role, and we define it as

$$\kappa(\omega) = (\max_i z(\omega_i) - \min_i z(\omega_i)). \tag{3.2}$$

Lastly, the projected polygon $P\omega$ may intersect itself in the plane Π_0. If there are m points on ω (for definiteness, only consider vertices and midpoints of edges) which are projected onto the same point of Π_0, then count this as $m-1$ intersections. Let the total number of these intersections of ω be

$$\mathscr{I}(\omega) = \text{number of intersections of } P\omega. \tag{3.3}$$

Since ω consists of n edges of length $\sqrt{2}$ joined at n vertices on the FCC, it is easy to check that

$$0 \leq \alpha(\omega) \leq n^2/8 \tag{3.4}$$

$$0 \leq \kappa(\omega) \leq n/2 \tag{3.5}$$

$$0 \leq \mathcal{I}(\omega) \leq 2n. \tag{3.6}$$

Note that these quantities are invariant under inversion of the lattice through the origin, and under lattice plane reflections and 45°-plane reflections of the lattice through planes perpendicular to Π_0. Therefore we can choose to leave the origin fixed by simply operating on the segment of ω not containing the origin in what follows, or we can always operate on the shorter of the two segments; all the lemmas will go through unchanged.

The next step is to prove that we can change (by performing a finite number of elementary transitions) any polygon ω into standard form. There are two cases that we shall consider separately. In the first case there exists a $z \in \mathcal{H}(\omega)$ which is not an element of $P\omega$. The second case are all those polygons such that $\mathcal{H}(\omega) \subset P\omega$ and there exists a point $z \in \mathcal{H}(\omega)$ which is the image of at least two vertices in $P\omega$. The only polygons not classified are those in standard form. Let us now consider these cases in turn.

(i) Suppose that there exists a point $z \in \mathcal{H}(\omega)$ such that $z \notin P\omega$. In the following D_z is a small open disc centred at z. Set up a cartesian coordinate system C with origin at z and x axis along the side of $\mathcal{H}(\omega)$ containing z. Choose the sign of the y axis such that all the points on $P\omega$ have zero or negative y coordinate. Let w_i and w_j be those vertices on ω, $i<j$, such that $P\omega_i$ and $P\omega_j$ are both on the x axis of C, such that the line segment $(P\omega_i, P\omega_j)$ contains z and such that the vertices $\{P\omega_{i+1}, P\omega_{i+2}, \ldots, P\omega_{j-1}\}$ all have negative y coordinates in C. In particular, all these vertices are off the x axis of C. With ω_i and ω_j as pivots, perform an inversion. The resulting polygon ω' is self-avoiding, since each point of $P[\omega_i : \omega_j]$, aside from the pivots, is reflected to a positive y coordinate in C, i.e. in $\mathrm{Ext}(\omega)$. Two things may happen with this pivot transition. Suppose that the curve $P[\omega_i : \omega_j]$ intersects the rest of the projected polygon $(P[\omega_j : \omega_i])$ (excluding $P\omega_i$ and $P\omega_j$). Then $\mathcal{I}(\omega')$ is less than $\mathcal{I}(\omega)$ by the number of such intersections. If there are no such intersections, then D_z is contained in $\mathrm{Int}(\omega')$. By the Jordan-Brouwer theorem (Greenberg and Harper 1981), the boundary of $\mathrm{Int}(\omega)$ must have been the union of the line segment $(P\omega_i, P\omega_j)$ with either $P[\omega_j : \omega_i]$ or $P[\omega_i : \omega_j]$; hence $(\mathrm{Int}(\omega') - D_z)$ contains either $\mathrm{Int}(\omega)$ or a rotated image of it. Thus, in the case that $\mathcal{I}(\omega)$ remains constant under the inversion, the area $\alpha(\omega)$ increases by at least the area of D_z.

(ii) We now assume that each point in $\mathcal{H}(\omega)$ is covered at least once by $P\omega$ and that there exists at least one point $z \in \mathcal{H}(\omega)$ which is the image of two vertices in ω, say, $z = P\omega_i = P\omega_j$ with $1 \leq i < j \leq n$. z is on one of the sides of the convex polygon $\mathcal{H}(\omega)$, and, by the geometry of Λ, this side is always parallel, or inclined at 45° to the principal axes ($\boldsymbol{e}_1$ or $\boldsymbol{e}_2$) in the plane Π_0 as set out before. Set up a cartesian coordinate system C on this side in the same manner as we have done above. There are three subcases to consider here.

Subcase a. $P[\omega_i : \omega_j]$ is contained in the x axis of C. By decreasing j if necessary, we can assume that $P\omega_i = P\omega_j = z$ and $P\omega_k \neq z$ for all $i < k < j$. Thus $P[\omega_i : \omega_j]$ is contained in either the positive x axis or the negative x axis. A 45°-plane reflection, or a 90°

rotation, with pivots ω_i and ω_j gives a self-avoiding polygon ω' with $P[\omega_i' : \omega_j']$ contained in the positive y axis of C. Recalling that the boundary of $P[\omega_i : \omega_j] \cup P[\omega_j : \omega_i]$ was a non-trivial convex polygon, it is not hard to see that $\mathscr{J}(\omega') < \mathscr{J}(\omega)$.

Subcase b. $P[\omega_j : \omega_i]$ is contained in the x axis of C. This is exactly analogous to subcase a.

Subcase c. Neither $P[\omega_i : \omega_j]$ nor $P[\omega_j : \omega_i]$ is contained in the x axis of C. Choose u and v such that $i \leq u < v \leq j$; $P\omega_u$ and $P\omega_v$ both have y coordinate zero (perhaps $P\omega_u \neq P\omega_v$); and $P\omega_k$ has negative y coordinate whenever $u < k < v$. With pivots ω_u and ω_v, perform an inversion. The resulting polygon, ω', must be self-avoiding, as argued in case (i), with $\mathscr{J}(\omega') \leq \mathscr{J}(\omega)$. We shall be happy if the number of intersections decreases, so assume that $\mathscr{J}(\omega') = \mathscr{J}(\omega)$. On the one hand, if $P\omega_u \neq P\omega_v$, then $\alpha(\omega') > \alpha(\omega)$ (since the union of the line segment $(P\omega_u, P\omega_v)$ with $P[\omega_u : \omega_v]$ has an interior of positive area, as does the union of $(P\omega_u, P\omega_v)$ and $P[\omega_v : \omega_u]$). On the other hand, if $P\omega_u = P\omega_v$, then $P[\omega_u' : \omega_v']$ and $P[\omega_v' : \omega_u']$ are curves which intersect in a single point, and which cannot both be line segments (since $P\omega$ was a non-trivial convex polygon); therefore ω' must belong to case (i) above.

Taking these cases now together we have the following lemma.

Lemma 3.3. Let ω be a polygon not in standard form and not contained in any plane. Then we can find pivots on ω and perform an inversion, or either a 45°-plane reflection or a 90° rotation, or two successive inversions, to find a polygon ω' with either (i) $\alpha(\omega') > \alpha(\omega)$, and $\mathscr{J}(\omega') \leq \mathscr{J}(\omega)$, or (ii) $\mathscr{J}(\omega') < \mathscr{J}(\omega)$ and $0 \leq \alpha(\omega') \leq n^2/8$.

Lemma 3.4. Let ω be any polygon, not flat (as defined in section 3.1) or not contained in a vertical plane. Then by performing inversions and either 45°-plane reflections or 90° rotations, we can pivot ω into a polygon in standard form. Furthermore, we need no more than n^3 transitions to complete this task.

Proof. We apply lemma 3.3, either reducing $\mathscr{J}(\omega)$ with each pivot, or increasing $\alpha(\omega)$ in at most two consecutive transitions. Since $\mathscr{J}(\omega)$ and $\alpha(\omega)$ are bounded as in (3.4) and (3.6), and since $2\alpha(\omega)$ must be an integer, it is easy to see that after at most n^3 transitions both these quantities will reach their maxima. □

It remains to show the following result.

Lemma 3.5. Every polygon in standard form can be transformed via a finite number of transitions into a flat polygon.

Proof. We say that a side of $\mathscr{H}(\omega)$ is 'diagonal' if it is inclined at 45° to the $\boldsymbol{e}_1$ and $\boldsymbol{e}_2$ axes; otherwise, the side must be parallel to one of the axis, and we say that the side is 'non-diagonal'.

To outline our strategy, define four classes of polygons:

$S_1 = \{\omega | \omega$ is in standard form and $\kappa(\omega) \geq 1\}$

$S_2 = \{\omega | \omega$ is in standard form and $\kappa(\omega) = 1\}$

$S_3 = \{\omega | \omega$ is in standard form, $\kappa(\omega) \leq 1$, and all non-diagonal sides (if any) of $\mathscr{H}(\omega)$ have length 1$\}$

$S_4 = \{\omega | \omega$ is a flat polygon$\}$.

We will show that every polygon in S_i can be transformed into a polygon in S_{i+1} for $i = 1, 2, 3$.

S_1 to S_2. Suppose that $\omega \in S_1$ and $\kappa(\omega) \geq 2$. Let $M = \max_j \{z(\omega_j)\}$. Choose i, j such that $z(\omega_i) = z(\omega_j) = M - 1$ and $[\omega_{i+1} : \omega_{j-1}]$ is contained in the plane $z = M$. With ω_i and ω_j as pivots, perform a reflection through the lattice plane $z = M - 1$. After at most $n^2/4$ repetitions of this procedure, we will obtain a polygon in S_2.

S_2 to S_3. Suppose that $\omega \in S_2$ and $P[\omega_i : \omega_j]$ is a non-diagonal side of $\mathcal{H}(\omega)$ having length 2 or more. Since $\kappa(\omega) = 1$, each consecutive pair of edges in $[\omega_i : \omega_j]$ must be mutually perpendicular. On the one hand, if $P[\omega_i : \omega_j]$ has even length, then a 45°-plane reflection, or a 90° rotation, with pivots ω_i and ω_j (into $\mathrm{Ext}(\omega)$), followed by $\frac{1}{2}(j-i)-1$ inversions with pivots ω_{i+1} and ω_{j-1}, and ω_{i+2} and ω_{j-2}, and so on, yields a polygon in standard form with one less non-diagonal side than ω (see figure 3). On the other hand, if $P[\omega_i : \omega_j]$ has odd length (≥ 3), then apply the above procedure to $[\omega_i : \omega_{j-1}]$, followed by an inversion with pivots $\omega_{(i+j-1)/2}$ and ω_j, yielding a polygon in standard form with a non-diagonal edge of length 1 (see figure 4).

S_3 to S_4. Let $\omega \in S_3$. If $P[\omega_i : \omega_j]$ is a diagonal side of $\mathcal{H}(\omega)$, then $[\omega_i : \omega_j]$ must lie in a plane parallel to Π_0; if $P[\omega_k : \omega_{k+1}]$ is a non-diagonal side, then $|z(\omega_k) - z(\omega_{k+1})| = 1$. It follows that the number of non-diagonal sides must be even (0, 2 or 4). If $\mathcal{H}(\omega)$ has zero non-diagonal sides, then ω is already in S_4.

If $\mathcal{H}(\omega)$ has exactly two non-diagonal sides, and they are not parallel (see figure 5), then it can be seen that n must be odd, and that a flat polygon can be obtained with one inversion (figure 5(b)).

Before we continue, let us consider a small example: $n = 4$, $\omega_1 = (1, 1, 0)$, $\omega_2 = (1, 2, 1)$, $\omega_3 = (0, 1, 1)$ and $\omega_4 = (0, 0, 0)$ (see figure 6(a)). This can be transformed in a flat polygon ω' with $\omega'_1 = (1, 1, 0)$, $\omega'_2 = (0, 2, 0)$, $\omega'_3 = (-1, 1, 0)$, $\omega'_4 = (0, 0, 0)$ (see

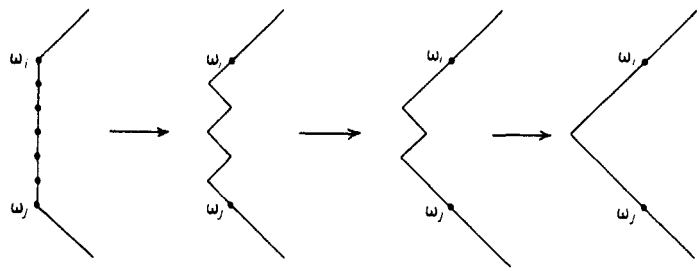

Figure 3. $P[\omega_i : \omega_j]$ has even length and is a non-diagonal side of $\mathcal{H}(\omega)$. With ω_i and ω_j as pivots, a 45°-plane reflection, or a 90° rotation, followed by a series of inversions will unfold the polygon as shown.

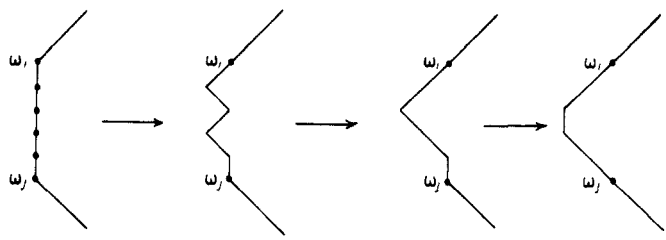

Figure 4. $P[\omega_i : \omega_j]$ has odd length and is a non-diagonal side of $\mathcal{H}(\omega)$. The series of transitions in figure 3 with ω_i and ω_{j-1} as pivots unfolds the polygons as shown. The last step is an inversion which puts the polygon back into standard form.

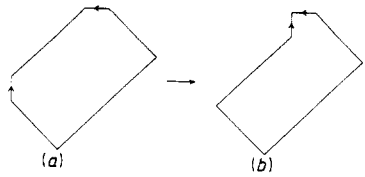

Figure 5. A polygon with an odd number of edges in the set S_3 can be made flat by a single inversion. The arrows indicate the direction in which z increases.

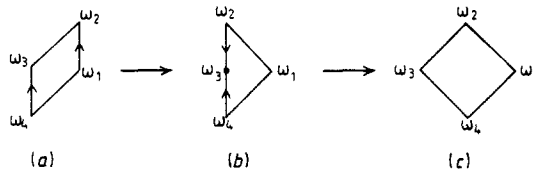

Figure 6. The polygon with four edges can be folded flat by using only 45°-plane reflections as indicated here. It is also possible to use inversions and 90° rotations.

figure 6(c)) in two pivots, as follows. First, with pivots ω_1 and ω_3, reflect through the 45° plane determined by (1, 1, 0), (0, 1, 1) and (0, 0, 1) (figure 6(b)). Then perform a second 45°-plane reflection with pivots ω_2 and ω_4. We can also perform this in three transitions, using a lattice-plane reflection, an inversion and a 90° rotation, as can be checked by the reader.

Now we return to the main task. If $\mathscr{H}(\omega)$ has exactly two non-diagonal sides, and they are parallel (see figure 7(a)), then n must be even. Two inversions (figure 7(b)), followed by the method of the above example yields a flat polygon (figure 7(c)).

Finally, if $\mathscr{H}(\omega)$ has four non-diagonal sides (figure 8(a)), then n must be even. Since $\kappa(\omega) = 1$, the edges whose projections onto Π_0 are parallel cannot themselves be parallel in $\mathbb{R}^3$ (e.g. the leftmost and rightmost edges in figure 8(a)). Then three inversions (figure 8(b)), followed by applying the example above yields a flat polygon. □

We have now finished the proof, and all that remains is to take together the results of lemmas 3.1, 3.4, 3.5 and 3.6.

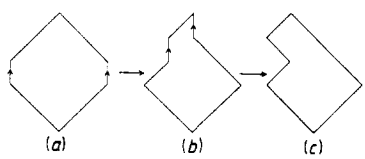

Figure 7. A polygon in S_3 with precisely two non-diagonal sides which are parallel. It can be folded flat by an inversion and the example in figure 6.

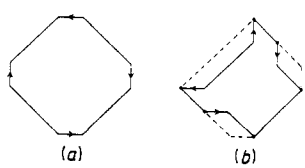

Figure 8. A polygon in S_3 with four non-diagonal sides. Three inversions and the example in figure 6 can be used to fold it into a flat polygon.

Theorem 3.6. The pivot algorithm applied to polygons is ergodic on the FCC lattice, providing that we give inversions, lattice plane reflections and either 45°-plane reflections or 90° rotations, positive probability of occurrence as elementary transitions in the Monte Carlo program.

4. Initialisation and numerical testing

The algorithm was programmed on an Apollo 10000 in FORTRAN77. We calculated the mean acceptance rate, the mean incidence of inversions, of lattice plane reflections, of 45°-plane reflections, and of 90° rotations. We define the square radius of gyration of a polygon ω to be

$$r^2(\omega) = \frac{1}{n}\sum_{i=1}^{n}[(x(\omega_i)-\bar{x})^2+(y(\omega_i)-\bar{y})^2+(z(\omega_i)-\bar{z})^2] \tag{4.1}$$

where $(\bar{x}, \bar{y}, \bar{z})$ is the centre of mass of the polygon, and define the span of a polygon to be

$$s(\omega) = \tfrac{1}{3}(\max_{i,j}\{|x(\omega_i)-x(\omega_j)|\}+\max_{i,j}\{|y(\omega_i)-y(\omega_j)|\}+\max_{i,j}\{|z(\omega_i)-z(\omega_j)|\}). \tag{4.2}$$

We calculated the mean square radius of gyration, $\langle r^2\rangle$, the mean fourth power of the radius of gyration, $\langle r^4\rangle$, the mean span, $\langle s\rangle$ and the mean of the square span divided by the square radius of gyration, $\langle s^2/r^2\rangle$. We also calculated the autocorrelations of the last four quantities. The values of n were taken such that $\log n$ increases roughly linearly in steps of 0.25.

4.1. Initialisation

In this section we discuss the initialisation of the MC program. We start the algorithm at an arbitrary configuration and discard the first T iterations, choosing T sufficiently large that we are confident that when we start to take observations, the process is near equilibrium. In this paper we start all our runs from a square configuration.

To estimate a magnitude for T we studied two global quantities associated with polygons, the mean span and the mean square radius of gyration. We performed a run with $n = 2981$, the longest polygons considered in this study. As the initial configuration we chose a square in the FCC. The mean span and mean square radius of gyration were calculated over blocks of 1000 iterations each, and after roughly 20 000 iterations these block averages are fluctuating about the mean. In this paper T was usually put equal to 150 000.

We performed a number of short runs to test the method and the program code. The results of these runs should agree with known values in the literature. For the FCC lattice, the exact enumeration study of Rapaport (1975) is useful in this respect. We discarded the first 20 000 observations before we took 100 000 observations for polygons with n between 5 and 12. The results showed exceptionally good agreement with Rapaport's values. For example for $n = 9$ we found $\langle r^2\rangle = 1.130(8)$ while Rapaport found 1.128 753.

4.2. Elementary transformations and acceptance fraction

Pivots were selected with uniform probability on the polygons. With a given selected pair of pivots it is possible to perform a number of elementary transformations, as

explained in subsection 2.1. In this study we chose the elementary transformations with uniform probability, i.e. if there are N possible transformations then each would be chosen with probability $1/N$.

The first feature of the elementary transformations we consider is the proportion of proposed transformations which are of type t, where $t = \mathrm{i}$ for inversions, $t = \mathrm{p}f$ for plane reflections, $t = \mathrm{p45}$ for 45°-plane reflections and $t = \mathrm{r90}$ for 90° rotations. Let g_t, $t = \mathrm{i}$, pf, p45 or r90, be the fraction of proposed transformations which are of type t. We plot g_t in figure 9(a) for each of the four kinds of transformations. For small n most proposed transformations are 45°-plane reflections, but this is soon overtaken by inversions as we increase n. Assume that $g_t \sim n^{-r_t}$, where r_t is an exponent. Since plane reflection can only take place if the pivots are selected on the same plane, we expect that $r_t = \nu$ for $t = \mathrm{p}f$ or $t = \mathrm{p45}$. (We assume that the polygon fills a spherical volume of radius n^{ν}.) Two-parameter least-squares fits to our data indicate that there are large corrections to this assumed simple scaling form. For $t = \mathrm{p}f$ or p45 we find r_t near 0.52, but with a very large systematic error (the exponent is strongly dependent on the choice of the minimum value of n in our data, the value above corresponds to a choice of the minimum value of n at 191). The same situation is apparent for $t = \mathrm{r90}$. The scaling assumption above is inadequate, and a more careful analysis, taking into account correlations between the vertices, is necessary to find the correct scaling law for g_t.

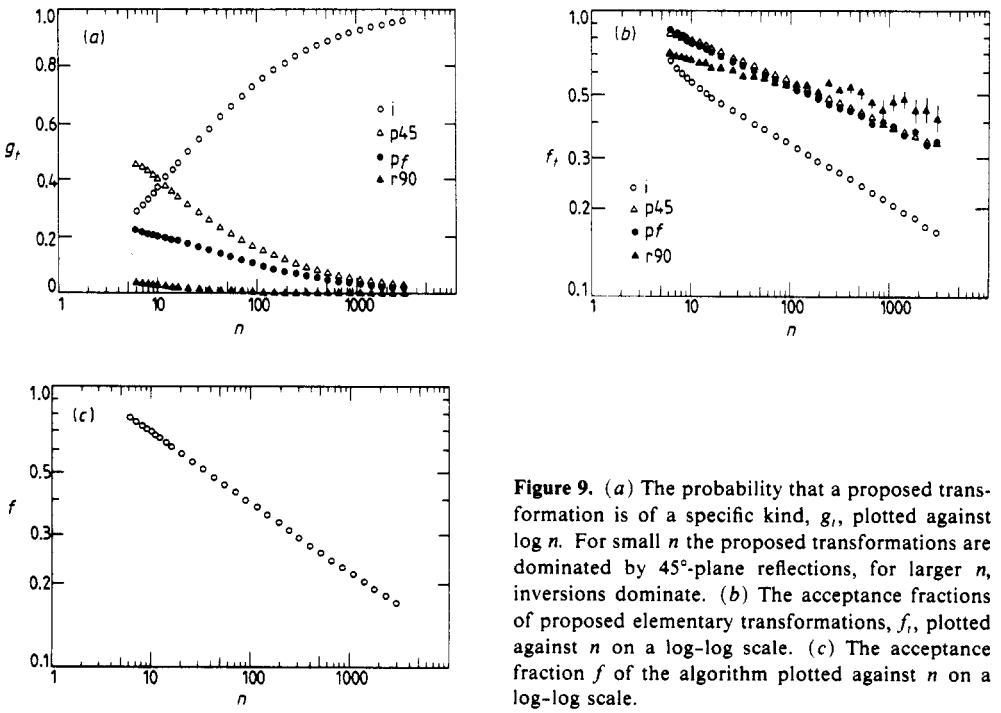

Figure 9. (a) The probability that a proposed transformation is of a specific kind, g_t, plotted against log n. For small n the proposed transformations are dominated by 45°-plane reflections, for larger n, inversions dominate. (b) The acceptance fractions of proposed elementary transformations, f_t, plotted against n on a log-log scale. (c) The acceptance fraction f of the algorithm plotted against n on a log-log scale.

The second property of the elementary transformations is the acceptance fraction of each of the different kinds of transformations. For example, if the transformation of type t is proposed, what is the probability, f_t, that it will be accepted? We plot f_t for $t = \mathrm{i}$, pf, p45 and r90 on a log-log scale in figure 9(b). These plots are straight

lines and we can assume that $f_t \sim n^{y_t}$, where y_t is an 'elementary transition exponent'. Two-parameter linear least-square fits to the data give $y_i = -0.206 \pm 0.001 \pm 0.001$, $y_{pf} = -0.145 \pm 0.005 \pm 0.003$, $y_{p45} = -0.153 \pm 0.003 \pm 0.001$ and $y_{r90} = -0.060 \pm 0.010 \pm 0.009$ for the exponents.

The values of y_t are given in the format value ± systematic error ± statistical error. The value of any parameter calculated by a least-squares analysis depends on the minimum length, n_{min}, (of the polygons) in the data; we compensate for this by introducing a systematic error in the following way. We increase n_{min} until we are satisfied that the estimate of the parameter has converged to an acceptable value, say at $n_{min} = m$. We then consider the successive results for $m < n_{min} < M$, where M is some cut-off (we chose $M = 191$). The largest difference between our best estimate and the successive results is then taken as the systematic error. This procedure is crude, but has the advantage that should we choose m too small, then we will find a large systematic error in our results (since correction to scaling will spoil the least-squares fit). The value of n_{min} is chosen, if possible, by increasing it until the parameters are within the 95% confidence intervals of estimates with larger n_{min}. Then we can assume that any increase in n_{min} will not give an improved estimate of the parameter. The statistical errors will always be 95% confidence limits. The error analysis will be performed in this way for the rest of this paper.

We see that, as a general rule, inversions have the least favourable dependence on n. For large n, inversions will dominate the proposed transitions, but will be less likely to be successful elementary transitions. The 90° rotations are much more likely to be successful, if proposed, than plane reflections or inversions in the large-n region. The fact that $y_p = y_{p45}$ is not a surprise. Both transitions are reflections through planes and depend similarly on the symmetry of the FCC lattice (i.e. operate on only one of the three components of the segment of the polygon that is reflected).

The acceptance fraction of the algorithm plays a major role in the effectiveness of MC programs. In particular, a MC algorithm can be rendered useless if the acceptance fraction of proposed elementary transitions is so low for the chosen input parameter, n, that we have to use large amounts of computer time to sample the system properly. The acceptance fraction is the number of successful elementary transformations divided by the total number of attempts. If the incidence of a proposed transition t is g_t, and its acceptance fraction is f_t, then $f = \Sigma_t g_t f_t$ is the acceptance fraction of the algorithm.

While it is known that the acceptance fraction f goes to zero as n goes to infinity, it seems that it will do so very slowly with increasing n, and that the algorithm will still be very effective, even for large values of n. In figure 9(c) we see that f is very large for small n; if $n = 6$ then f is in the order of 0.8, and it decreases very slowly to about 0.2 if $n = 2981$. This means that even for these long polygons, roughly one of every five proposed transitions is successful.

A log-log plot of f against n (figure 9(c)) is linear. We therefore expect a simple power-law dependence of f on n. An ansatz that

$$f = c_0 n^{-p} \tag{4.3}$$

and a two-parameter least-squares fit to the data gives

$$p = 0.247 \pm 0.004 \pm 0.001 \qquad c_0 = 1.22 \pm 0.03 \pm 0.01. \tag{4.4}$$

To illustrate that there is virtually no concavity in the plot due to values of f at small n (and thus no significant corrections to scaling) we discarded all data points to $n = 70$

and repeated the least-squares analysis. We found $p = 0.245 \pm 0.003 \pm 0.001$ and $c_0 = 1.20 \pm 0.03 \pm 0.01$. There is very little numerical evidence of any significant corrections to (4.6). This correlates with the results of Madras and Sokal (1988) for the pivot algorithm and the self-avoiding walk. The relation between p and the critical exponents of polygons is unknown; it is not even known whether p is universal (see appendix A in Madras and Sokal 1988). For the self-avoiding walk on the cubic lattice Madras and Sokal (1988) report that $p_w = 0.107$, which is quite different from the result here.

4.4. Work

In this section we consider the 'computational efficiency' of the algorithm. We consider two quantities. The first is the mean number of operations that we must perform per pivot, and the second is the mean number of operations per successful pivot.

There are several parts of the MC algorithm where the number of operations (amount of work) performed for each attempted pivot depends in some way on n. The choice of two pivots takes some computation, namely obtaining two random numbers and identifying the coordinates of the pivots, but is independent of the number of vertices in the polygon (since the coordinates of ω are stored in an array). In contrast to this, if we check a proposed configuration for self-intersections, then it seems plausible to suppose that the number of vertices to be checked does depend in some way on n. In our program we read vertices near the pivots first into the hash table. If a configuration intersects itself, then we believe that it will mostly be near the pivots. Madras and Sokal (1988) claim that by using this scheme, the rejection of intersecting configurations will take $O(n^{1-p_w})$ operations, but every successful transition will take $O(n)$ operations. In our algorithm we identified several sources of 'work'. Once we have chosen two pivots, say r_1 and r_2, they are: proposing a new configuration, checking that it is self-avoiding, and resetting the hash table. Finally, if the proposed configuration is accepted, then updating the old configuration is another source of work.

In order to check the computational efficiency of the algorithm, we performed a series of short runs (50 000 iterations) and measured the amount of work. The results are set out in table 1. Consider first the results of work per attempted pivot. It seems reasonable to propose a dependence

$$\text{work per attempted pivot} = C_0 n^w \tag{4.5}$$

where w is a 'work-exponent' of the MC algorithm. To test this hypothesis we plotted the work per attempted pivot against n on a log–log scale. The plot is linear. A two-parameter least-squares fit to the data in table 1 gives (for the parameters in (4.5))

$$w = 0.858 \pm 0.001 \pm 0.002 \qquad C_0 = 2.88 \pm 0.03 \pm 0.04. \tag{4.6}$$

Since a successful transition occurs roughly every f^{-1} iterations, we expect from (4.3) and (4.5) that

$$\text{work per successful transition} = C_0 n^{w+p} \tag{4.7}$$

where $w + p \approx 1.105 \pm 0.008$ (we add the systematic and statistical errors). A least-squares fit to the second set of data in table 1 gives

$$w + p = 1.099 \pm 0.003 \pm 0.002 \qquad C_0 = 2.46 \pm 0.06 \pm 0.03 \tag{4.8}$$

close to the expected values. On the square lattice for random walks Madras and Sokal (1988) report that the mean work per successful pivot is about $O(n)$. That is better than the $O(n^{w+p})$ found here.

Table 1. The average work per pivot, the average work per successful pivot and the acceptance frequency f as functions of the polygon length n.

n	Work/Pivot	Work/(Successful pivot)	f
6	11.93 (2)	15.28 (3)	0.7807 (3)
7	13.86 (2)	18.41 (4)	0.7530 (3)
8	15.93 (3)	21.80 (5)	0.7307 (3)
9	17.98 (3)	25.25 (5)	0.7119 (3)
10	19.71 (3)	28.41 (6)	0.6938 (3)
12	23.53 (4)	35.53 (8)	0.6623 (3)
16	32.11 (6)	52.1 (1)	0.6159 (3)
20	37.79 (8)	64.8 (1)	0.5836 (4)
26	48.6 (1)	89.0 (3)	0.5458 (4)
33	60.1 (1)	116.8 (4)	0.5144 (4)
43	73.4 (2)	152.6 (5)	0.4809 (4)
55	98.1 (3)	217.1 (7)	0.4519 (4)
70	111.8 (3)	262.6 (9)	0.4257 (4)
90	138.6 (4)	347 (1)	0.3994 (4)
116	172.6 (5)	458 (2)	0.3767 (3)
148	211.1 (7)	598 (3)	0.3534 (3)
191	262.9 (9)	791 (4)	0.3325 (3)
245	331 (1)	1 062 (5)	0.3125 (3)
314	397 (1)	1 352 (6)	0.2934 (3)
403	492 (2)	1 783 (9)	0.2758 (3)
518	609 (2)	2 340 (10)	0.2603 (3)
665	750 (3)	3 070 (20)	0.2440 (3)
854	930 (4)	4 030 (20)	0.2309 (3)
1097	1155 (5)	5 340 (30)	0.2163 (3)
1408	1424 (6)	6 700 (40)	0.2036 (3)
1808	1801 (8)	9 400 (60)	0.1916 (3)
2322	2290 (10)	12 610 (80)	0.1814 (3)
2981	2850 (10)	16 800 (100)	0.1701 (3)

5. Numerical results

5.1. Autocorrelation functions

In order to give error bars on quantities calculated in a MC study like this, we must calculate the autocorrelation functions of several observables (see subsection 2.2). Since the algorithm simulates polygons when the Markov chain is almost stationary, it is the integrated autocorrelation times (equation (2.7)) in which we are interested.

It is difficult to calculate quantities like the autocorrelation functions by a means of a MC calculation. Noise in the data soon makes any measurement unreliable. From a sample size of N observations, the *natural* estimator of (2.7) is

$$\hat{\tau}_{\mathrm{int}}(A) = \frac{1}{2}\sum_{t=-(N-1)}^{N-1}\left(C_{AA}^{-1}(0)\frac{1}{N-|t|}\sum_{i=1}^{N-|t|}(A_i - A)(A_{i+|t|} - A)\right)$$

$$= \frac{1}{2}\sum_{t=-(N-1)}^{N-1}\hat{\rho}(t). \tag{5.1}$$

A is the sample mean of an observable $\mathscr{A}$ which is measured after each iteration, producing a random sequence of estimates $\{A_i\}$. Because $\hat{\rho}(t)$ is mostly noise when t is large, it is much better to use a 'window' $\lambda(t)$ in (5.1), where $\lambda(t) \approx 1$ if $|t| \leqslant \tau_{\mathrm{int}}$,

and 0 otherwise. We calculated τ_{int} using this approach. A batch job of mN iterations was divided into m blocks of N iterations each, where $N \gg \tau_{\text{int}}$. τ_{int} is then calculated for each of the m blocks, using equation (5.1). The window $\lambda(t)$ was defined in the following way. Let t_0 be the largest number such that $\hat{\rho}(t) \geqslant 0$ for all $t \leqslant t_0$. Then $\lambda(t) = 1$ for all $t \leqslant t_0$ and 0 otherwise. In particular, even though $\rho(t) \geqslant 0$, we found in practice that a statistical measurement of ρ may be negative if we increase t. Thus if we write

$$\hat{\tau}_{\text{int}}(A) = \frac{1}{2} \sum_{t=-(N-1)}^{N-1} \lambda(t) \hat{\rho}_{AA}(t) \tag{5.2}$$

then we only add all those terms up to the first negative term. Since we bias (5.2) in favour of terms with positive noise, we expect that this procedure will produce a slight overestimate of the autocorrelations.

Since we have assumed that $N \gg \tau_{\text{int}}$, we can assume that each of the m blocks of data is producing an independent estimate of τ_{int} (we chose N at least $100\tau_{\text{int}}$, and in general much larger). Therefore we can calculate a mean autocorrelation time by simply taking an average over the blocks of data. The first autocorrelation calculated was that of the acceptance fraction f. Over 50 000 iterations we put $N = 250$ and $m = 200$ in the above analysis. We found that $\tau_{\text{int}}(f)$ decreases in general with increasing n, from $\tau_{\text{int}}(f) = 0.70 \pm 0.02$ for $n = 6$ to $\tau_{\text{int}}(f) = 0.63 \pm 0.01$ for $n = 2981$ (95% confidence limits). This short autocorrelation time indicates that the acceptance or rejection of a particular proposed configuration is weakly dependent on whether the last transition was successful.

The autocorrelation times of the elementary transitions were calculated in the same runs. If we calculate the incidence of inversions by putting $i = 1$ if an inversion was successful and 0 otherwise, then $\tau_{\text{int}}(i)$ decreases steadily from 0.65 ± 0.02 for $n = 6$ to 0.64 ± 0.02 for $n = 2981$. Similarly, we can calculate the autocorrelations of the other elementary transitions; they are all short (no bigger than 0.7) and tend to decrease as n is increased.

Of greater interest to us are the autocorrelations of global properties like the span and the mean square radius of gyration. To this end, we chose $N = 10\,000$ and $m = 50$ and calculated the autocorrelations of the mean square radius of gyration ($\tau_{\text{int}}(r^2)$), the mean span ($\tau_{\text{int}}(s)$), the mean fourth power radius of gyration ($\tau_{\text{int}}(r^4)$) and the mean of the ratio of the square span and square radius of gyration ($\tau_{\text{int}}(s^2/r^2)$). ($N = 1000$ was found to be too small; increasing it to 10 000 increased the estimates of the autocorrelations significantly for $n = 2981$. Increasing N to 20 000 did not produce estimates significantly different from those at 10 000. We concluded, therefore, that 10 000 is a suitable choice for N.) The results are plotted in figure 10.

It is reasonable to expect that the autocorrelation of a global quantity should be inversely proportional to the acceptance fraction f. In fact, we expect that after every few successful transitions that we will find a new 'independent' configuration. From equation (4.3) and figure 10 we postulate that

$$\tau_{\text{int}}(A) = C_0 n^{q(A)} \tag{5.3}$$

where $q(A)$ is an exponent, possibly different for each global observable and where we expect that $q(A) \geqslant p$. A two-parameter least-squares fit to the data gives

$$\begin{aligned} q(r^2) &= 0.27 \pm 0.02 \pm 0.02 & q(r^4) &= 0.31 \pm 0.02 \pm 0.02 \\ q(s) &= 0.29 \pm 0.03 \pm 0.02 & q(s^2/r^2) &= 0.23 \pm 0.02 \pm 0.02. \end{aligned} \tag{5.4}$$

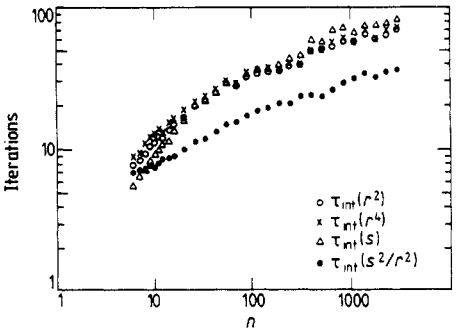

Figure 10. Autocorrelation times of global observables. For $n \geq 70$ the curves flatten out to become roughly linear.

These results are all, within statistical error, greater than p. The small values of $q(A)$ implies that $\tau_{\text{int}}(A)$ increases slowly with n, making the algorithm particularly useful for the simulation of long polygons.

5.2. *The mean square radius of gyration and the mean span*

The results from our main MC runs are summarised in table 2. We calculated the mean square radius of gyration, $\langle r^2 \rangle_n$, the mean fourth power of the radius of gyration, $\langle r^4 \rangle_n$, the mean span, $\langle s \rangle_n$, and the mean square span divided by the mean square radius of gyration, $\langle s^2/r^2 \rangle_n$, for n ranging from 6 to 2981 spaced such that log n is incremented by 0.25 from approximately 1.75 to 8.00.

5.2.1. Mean square radius of gyration. The mean square radius of gyration of polygons on the FCC was considered by Rapaport (1975), using an exact enumeration scheme. In general it is believed that $\langle r^2 \rangle_n$ should scale as a simple power law with n, but it is known that strong corrections can be expected to this behaviour (Wegner 1972). From field theoretic considerations (Le Guillou and Zinn-Justin 1980, 1989) it seems reasonable to suspect that

$$\langle r^2 \rangle_n = n^{2\nu}(A + Bn^{-\Delta} + Cn^{-1} + o(n^{-1})) \tag{5.5}$$

where A, B and C are lattice-dependent constants, while Δ is the correction-to-scaling exponent. This form allows for both an analytic and a non-analytic correction to scaling.

Ideally, one would like to estimate the five parameters in (5.5) directly from the MC data without further assumptions. However, the data are not sufficiently accurate to make this viable; in general it is found that the numerical procedures are unstable. We begin, therefore, by estimating ν by plotting $\langle r^2 \rangle_n$ against n on a log-log scale in figure 11. The plot is linear and suggests that a least-squares fit will produce 2ν. Our best estimates are

$$\nu = 0.593 \pm 0.003 \pm 0.002 \qquad A = 0.167 \pm 0.020 \pm 0.001. \tag{5.6}$$

The value for ν compares well with results in the literature; Madras and Sokal (1988) found 0.592 ± 0.003 for the self-avoiding walk by using the pivot algorithm. The series analysis method of Guttmann (1987) gives 0.592 ± 0.002 while Rapaport (1975) found 0.592 ± 0.004.

Although all these numerical estimates agree to a high accuracy, they are all systematically larger than the field theory estimates of Le Guillou and Zinn-Justin (1980, 1989) ($\nu = 0.588 \pm 0.002$ and $\Delta = 0.470 \pm 0.025$). An examination of the curve

Table 2. The values of global quantities calculated with the pivot algorithm.

n	Number of iterations	$\langle r^2 \rangle$	$\langle r^4 \rangle$	$\langle s \rangle$	$\langle s^2/r^2 \rangle$
6	4.0×10^6	1.418 (2)	2.568 (5)	1.8412 (3)	2.5928 (8)
7	2.5×10^6	1.696 (3)	3.73 (1)	2.0756 (7)	2.780 (1)
8	2.5×10^6	1.976 (3)	5.130 (2)	2.3125 (5)	2.949 (1)
9	2.5×10^6	2.258 (4)	6.80 (3)	2.5397 (3)	3.087 (1)
10	2.5×10^6	2.550 (5)	8.75 (3)	2.7514 (5)	3.207 (1)
11	2.5×10^6	2.896 (6)	$1.138\,(4)\times10^1$	2.9907 (6)	3.325 (1)
12	2.5×10^6	3.150 (6)	$1.351\,(5)\times10^1$	3.1605 (7)	3.401 (1)
14	2.5×10^6	3.772 (7)	$1.955\,(8)\times10^1$	3.538 (1)	3.559 (1)
16	2.5×10^6	4.407 (9)	$2.69\,(1)\times10^1$	3.894 (2)	3.688 (1)
20	2.5×10^6	5.74 (2)	$4.60\,(2)\times10^1$	4.570 (2)	3.887 (2)
26	2.5×10^6	7.84 (2)	$8.65\,(5)\times10^1$	5.483 (2)	4.097 (2)
33	2.5×10^6	$1.041\,(3)\times10^1$	$1.53\,(1)\times10^2$	6.446 (2)	4.263 (2)
43	2.5×10^6	$1.426\,(4)\times10^1$	$2.89\,(2)\times10^2$	7.693 (3)	4.432 (2)
55	2.5×10^6	$1.912\,(6)\times10^1$	$5.22\,(3)\times10^2$	9.045 (4)	4.572 (2)
70	2.5×10^6	$2.547\,(8)\times10^1$	$9.32\,(6)\times10^2$	$1.059\,(5)\times10^1$	4.693 (2)
90	2.5×10^6	$3.44\,(1)\times10^1$	$1.70\,(1)\times10^3$	$1.2432\,(7)\times10^1$	4.805 (2)
116	2.5×10^6	$4.65\,(2)\times10^1$	$3.14\,(2)\times10^3$	$1.4619\,(7)\times10^1$	4.900 (2)
148	2.5×10^6	$6.21\,(2)\times10^1$	$5.60\,(4)\times10^3$	$1.7031\,(9)\times10^1$	4.986 (2)
191	2.5×10^6	$8.41\,(3)\times10^1$	$1.032\,(8)\times10^4$	$1.998\,(1)\times10^1$	5.066 (2)
245	2.5×10^6	$1.130\,(4)\times10^2$	$1.865\,(2)\times10^4$	$2.332\,(2)\times10^1$	5.132 (2)
314	2.5×10^6	$1.512\,(6)\times10^2$	$3.33\,(3)\times10^4$	$2.712\,(2)\times10^1$	5.193 (3)
403	2.5×10^6	$2.041\,(8)\times10^2$	$6.09\,(6)\times10^4$	$3.167\,(2)\times10^1$	5.246 (3)
518	2.5×10^6	$2.75\,(1)\times10^2$	$1.11\,(1)\times10^5$	$3.691\,(3)\times10^1$	5.292 (3)
665	2.5×10^6	$3.68\,(2)\times10^2$	$1.99\,(2)\times10^5$	$4.292\,(3)\times10^1$	5.338 (3)
854	2.5×10^6	$4.98\,(3)\times10^2$	$3.64\,(4)\times10^5$	$5.000\,(4)\times10^1$	5.368 (3)
1097	2.5×10^6	$6.65\,(4)\times10^2$	$6.51\,(6)\times10^5$	$5.809\,(5)\times10^1$	5.407 (3)
1408	2.5×10^6	$8.95\,(5)\times10^2$	$1.18\,(1)\times10^6$	$6.753\,(5)\times10^1$	5.438 (3)
1808	2.5×10^6	$1.199\,(6)\times10^3$	$2.11\,(2)\times10^6$	$7.843\,(7)\times10^1$	5.462 (3)
2322	2.5×10^6	$1.612\,(8)\times10^3$	$3.87\,(4)\times10^6$	$9.125\,(7)\times10^1$	5.486 (3)
2981	3.0×10^6	$2.17\,(1)\times10^3$	$6.95\,(9)\times10^6$	$1.059\,(9)\times10^2$	5.500 (3)

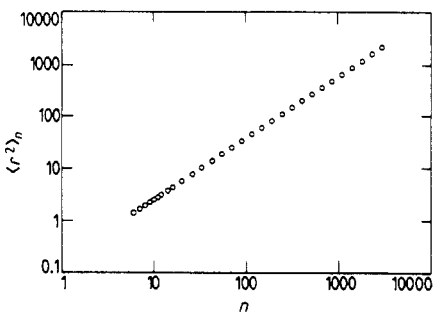

Figure 11. $\langle r^2 \rangle_n$ against n on a log-log scale. The error bars are too small to show up on this scale.

fitting procedure indicates that ν increases with $n_{\min}$ from 0.591 for $n_{\min}=6$, to 0.593 for $n_{\min}=55$, exposing a slight convexity in the curve in figure 11. This is also illustrated in a plot of $\langle r^2 \rangle_n / n^{2\nu}$ (where ν is given its MC value) against $1/n$ in figure 12(a). If we expect only an analytic correction to the assumed scaling form (5.5), then the plot should be linear. Instead we see a sharp curve for large n.

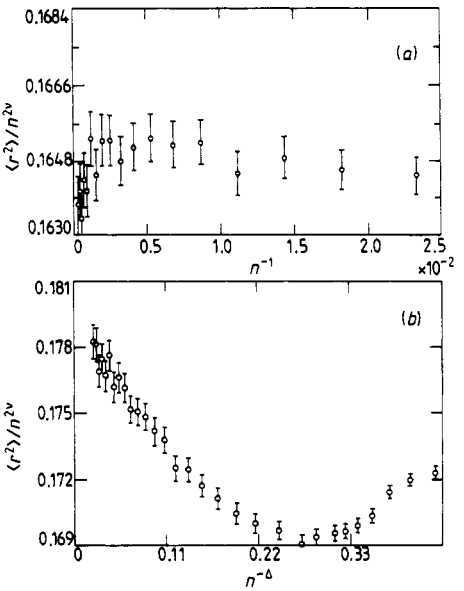

Figure 12. (*a*) $\langle r^2\rangle_n/n^{2\nu}$ against n^{-1} for $\nu = 0.593$. For small n the curve is roughly linear, but it curves sharply down as we increase n. This indicates that we are neglecting a confluent singularity which dominates the n^{-1} term for larger n. (*b*) $\langle r^2\rangle_n/n^{2\nu}$ against $n^{-\Delta}$ for $\nu = 0.588$. The curve goes through a minimum before it flattens out to become linear for larger n. This is strong evidence that a confluent correction to scaling of order $n^{-\Delta}$ is present in the data.

In figure 12(*b*), we plot $\langle r^2\rangle_n/n^{2\nu}$ against $n^{-\Delta}$ for the field theory values of the exponents. The plot is dramatically different from figure 12(*a*). For small n, it goes through a minimum, indicating that the analytic and non-analytic corrections have opposite signs in (5.5); as n is increased the plot becomes linear. We interpret this as strong support for equation (5.5) with the field theory values of the exponents. (Of course, small changes in these will not alter the curve significantly.) We can estimate the values of the coefficients in (5.5) by a linear least-squares fit (since we are interested in the corrections to scaling here, we choose $n_{\min} = 6$ and we do not attempt to find a systematic error):

$$A = 0.179 \pm 0.005 \qquad B = -0.0640 \pm 0.0006 \qquad C = 0.13 \pm 0.01 \tag{5.7}$$

where the errors are 95% confidence limits.

The mean fourth moment of the radius of gyration of polygons is expected to have scaling behaviour similar to that in equation (5.5). If we suppose that

$$\langle r^4\rangle_n = C' n^{\gamma_4} \tag{5.8}$$

then the results of Rapaport (1975) suggest that $\gamma_4 = 4\nu$. To test this, we performed a two-parameter least-squares fit to the data. We find

$$\gamma_4 = 2.375 \pm 0.004 \pm 0.004 \qquad C' = 0.0400 \pm 0.0004 \pm 0.0004 \tag{5.9}$$

close to the number $4\nu = 2.372 \pm 0.016$.

5.2.2. Mean span. The span of polygons and self-avoiding walks have received little attention in the literature (Bellemans 1973a, b, Privman and Rudnick 1985). If we

assume that there is only one length scale for polygons, then we can use the results from the mean square radius of gyration to assume that

$$\langle s\rangle_n = n^{\nu}(a + bn^{-\Delta} + cn^{-1} + o(n^{-1})). \tag{5.10}$$

A comparison of (5.5) and (5.10) suggests that

$$\langle s^2/r^2\rangle_n = \alpha + \beta n^{-\Delta} + \gamma n^{-1} + o(n^{-1}). \tag{5.11}$$

It is believed that α is a universal constant. For self-avoiding walks McCrackin *et al* (1973), Rapaport (1985) and Madras and Sokal (1988) studied the analogous situation for the mean end-to-end length and the mean square radius of gyration.

To study the assumption (5.11), we plotted $\langle s^2/r^2\rangle_n$ against $n^{-\Delta}$ in figure 13. The ratio appears to approach a finite value as we increase n. This implies that the exponent governing the large-n behaviour is identical for both the mean square span and the mean square radius of gyration. Moreover, the linear behaviour suggests that the field theoretic value of the confluent singularity fits the data well. There is no turning point in this curve, so we expect that the analytic correction term must have a small amplitude compared to the confluent term. A least-squares analysis gives

$$\alpha = 5.69 \pm 0.02 \qquad \beta = -7.50 \pm 0.01 \qquad \gamma = 0.6 \pm 0.1 \tag{5.12}$$

with 95% confidence limits and where α is a universal number.

Closely related to the ratio studied above is

$$\frac{\langle s\rangle^2}{\langle r^2\rangle} = \alpha' + \beta' n^{-\Delta} + \gamma' n^{-1}. \tag{5.13}$$

We expect that α' is also universal. We calculated the ratios from table 2. In (5.13) we calculated error bars by a triangle inequality. A least-squares analysis gives (95% confidence limits)

$$\alpha' = 5.3 \pm 0.2 \qquad \beta' = -6.9 \pm 0.1 \qquad \gamma' = -0.3 \pm 0.4. \tag{5.14}$$

These results strongly suggest that the exponents ν and Δ are universal. We can now perform the same analysis for the span as for $\langle r^2\rangle$ to determine numerical values from our data for ν. However, an attempt to perform a two-parameter linear fit to calculate ν fails because the corrections to scaling are too large. Assuming that $\langle s\rangle_n = an^{\nu}$ reveals that the parameters a and ν are so strongly dependent on the choice of $n_{\min}$ that we are unable to make a best estimate for the parameters as we have done from $\langle r^2\rangle$.

However, the MC data are consistent with the theoretical results of Le Guillou and Zinn-Justin (1980, 1989). A plot of $\langle s\rangle_n/n^{\nu}$ against $n^{-\Delta}$ (figure 14) is linear, suggesting

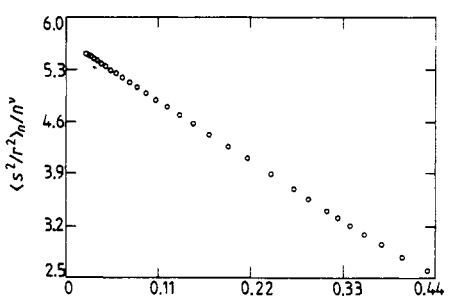

Figure 13. $\langle s^2/r^2\rangle_n/n^{\nu}$ against $n^{-\Delta}$ for $\nu = 0.588$. The line goes to a finite constant as $n \to \infty$. This constant is believed to be universal.

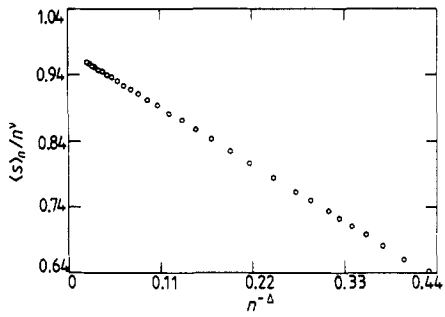

Figure 14. $\langle s \rangle_n / n^{\nu}$ against $n^{-\Delta}$ for $\nu = 0.588$. The linear nature of this plot suggests that $n^{-\Delta}$ takes care of virtually all the corrections to scaling in the mean span.

little analytic corrections to scaling. There is, however, as expected from the arguments above, a large confluent term. A least-squares analysis gives

$$a = 0.978 \pm 0.003 \qquad b = -0.798 \pm 0.001 \qquad c = 0.040 \pm 0.007 \tag{5.15}$$

with 95% confidence limits.

6. Conclusions

In this paper we considered the pivot algorithm for polygons on the face-centred cubic lattice. This algorithm has proved to be very effective for self-avoiding walks on the cubic lattice. We proved that the algorithm for polygons is ergodic on the FCC provided that we give a set of elementary transitions positive probability of occurrence. It is now known that the pivot algorithm for polygons is ergodic on the hypercubic (Madras *et al* 1989) and on the FCC lattice (this work). Little is known about other lattices such as the tetrahedral lattice, which has a different symmetry group from the cubic lattices.

The second major aim of this paper was to generate some numerical data on polygons in three dimensions. The numerical studies of polygons in the canonical ensemble in the past have been limited to exact enumeration and to generating polygons by simulating random walks. In the grand canonical ensemble most studies are limited to a local elementary transition (Berg and Foester 1981, Aragao de Carvalho *et al* 1983), an approach which suffers from long auto-correlation times (Sokal and Thomas 1988) and which is not ergodic, since it preserves the knot class of a polygon (Madras and Sokal 1987). These problems can both be overcome by supplementing the elementary transformations by a pivot transition, such as inversion (Caracciolo *et al* 1989).

The main conclusions we can draw from our work are the following.

(i) We found that the acceptance fraction of the pivot algorithm goes to zero slowly; $f \sim n^{-p}$. We found the value of p to be roughly $\frac{1}{4}$. This value is different from the analogous value for self-avoiding walks on the cubic lattice. It is not clear whether this difference is due to the lattice (that p is a lattice-dependent number), or due to the fact that we are dealing with polygons, or both. The relative incidence of the elementary transitions is important. We see that inversion dominates the transitions for large values of n; this fact is possibly partly responsible for the longer autocorrelation times that we see for longer walks (since inversions alone does not suffice for ergodicity). For smaller n, 45°-plane reflections dominate the transitions.

(ii) We defined a work exponent w as a measure of the computational efficiency of the algorithm. We found that the number of operations required to produce a new configuration is n^{w+p}, where $w+p \approx 1.1$. This is more than the $O(n)$ operations needed in the case of the self-avoiding walk, but is a vast improvement on previous efforts for polygons. The autocorrelations of the global quantities that we calculated (one effectively independent polygon for every eighty attempts at $n = 2981$) are very short, and we conclude that the algorithm is extraordinarily efficient in the simulation of polygons.

(iii) The numerical data are completely consistent with the expected values of the critical exponents from the literature. However, our analysis also indicates that a two-parameter fit to data containing corrections to scaling can be very deceptive. While we found that the parameters converge rapidly to values insensitive to $n_{\min}$ in the case of $\langle r^2 \rangle$, it is nevertheless not the field theory values that we find, even with polygons as long as those studied in this paper. To resolve this issue it is necessary to perform a five-parameter fit to (5.5), although there is no guarantee that this will work, since higher-order corrections to scaling may still contaminate the data to make this impossible. We do show, however, that the data presented here are completely consistent with field theory, provided that we take corrections to scaling into account.

(iv) With the span of the polygons we find that the confluent correction to scaling is so strong that it is not possible to perform a two-parameter fit to determine its associated scaling exponent. Figure 14 illustrates the dominance of the confluent term in the correction and this is borne out by the least-squares fit to find the amplitudes of the terms in (5.10). The span and the square radius of gyration do define the same length scale, as we see from figure 13. The ratio $\langle s^2/r^2 \rangle$ goes to a constant α as n goes to infinity. The number α is believed to be lattice independent.

Acknowledgments

This research was financially supported by NSERC of Canada. We thank Alan D Sokal for his helpful comments on this paper.

References

Aragao de Carvalho C, Caracciolo S and Fröhlich J 1983 *Nucl. Phys.* B **251** 209
Bellemans A 1973a *Physica* **73** 368
—— 1973b *Physica* **74** 441
Berg B and Foester D 1981 *Phys. Lett.* **106B** 323
Caracciolo S, Pelissetto A and Sokal A D 1990 *J. Stat. Phys.* **60** to be published
Dubins L E, Orlitsky A, Reeds J A and Shepp L A 1988 *IEEE Trans. Inform. Theory* **34** 1509
Enting I G and Guttmann A J 1989 *J. Phys. A: Math. Gen.* **22** 1371
Frank-Kamenetskii M D, Lukashin A V and Vologodskii A V 1975 *Nature* **258** 398
Freire J J and Horta A 1976 *J. Chem. Phys.* **65** 4049
Greenberg M J and Harper J R 1981 *Algebraic Topology* (Menlo Park, CA: Benjamin/Cummings)
Guttmann A J 1987 *J. Phys. A: Math. Gen.* **20** 1839
Guttmann A J and Enting I G 1988 *J. Phys. A: Math. Gen.* **21** L165
Hammersley J M 1961 *Proc. Camb. Phil. Soc.* **57** 516
Horowitz E and Sahni S 1976 *Fundamentals of Data Structures* (Potomac, MD: Computer Science Press)
Kemeny J G and Snell J L 1976 *Finite Markov Chains* (Berlin: Springer)
Kesten H 1963 *J. Math. Phys.* **4** 960
Knuth D E 1973 *The Art of Computer Programming* vol 3 (Reading, MA: Addison-Wesley)

Lal M 1969 *Molec. Phys.* **17** 57
Le Guillou J C and Zinn-Justin J 1980 *Phys. Rev.* B **21** 3976
—— 1989 *J. Physique* **50** 1365
MacDonald B, Jan N, Hunter D L and Steinitz M O 1985 *J. Phys. A: Math. Gen.* **18** 2627
Madras N, Orlitsky A and Shepp L A 1990 *J. Stat. Phys.* **58** 159
Madras N and Sokal A D 1987 *J. Stat. Phys.* **47** 543
—— 1988 *J. Stat. Phys.* **50** 109
Martin J L, Sykes M F and Hioe F T 1967 *J. Chem. Phys.* **46** 3478
McCrackin F L, Mazur J and Guttman C M 1973 *Macromolecules* **6** 859
Metropolis N, Rosenbluth A W, Rosenbluth M N, Teller A H and Teller E 1953 *J. Chem. Phys.* **21** 1087
Michels J P J and Wiegel F W 1986 *Proc. R. Soc.* A **403** 269
Olaj O F and Pelinka K H 1976 *Makromol. Chem.* **177** 3413
Privman V and Rudnick J 1985 *J. Phys. A: Math. Gen.* **18** L789
Rapaport D C 1975 *J. Phys. A: Math. Gen.* **8** 1328
—— 1985 *J. Phys. A: Math. Gen.* **18** 113
Sokal A D and Thomas L E 1988 *J. Stat. Phys.* **51** 907
Stellman S D and Gans P J 1972a *Macromolecules* **5** 516
—— 1972b *Macromolecules* **5** 720
Sumners D W 1987 *J. Math. Chem.* **1** 1
Wegner F J 1972 *Phys. Rev.* B **5** 4529